Nuclear Instruments and Methods in Physics Research B 409 (2017) 53–59

Contents lists available at ScienceDirect

Nuclear Instruments and Methods in Physics Research B

journal homepage: www.elsevier.com/locate/nimb

Homojunction silicon solar cells doping by ion implantation

Frédéric Milési [a,b,*], Marianne Coig [a,b], Jean-François Lerat [a,c], Thibaut Desrues [a,c], Jérôme Le Perchec [a,c], Adeline Lanterne [a,c], Laurent Lachal [a,b], Frédéric Mazen [a,b]

[a] Univ. Grenoble Alpes, F-38000 Grenoble, France
[b] CEA, LETI, MINATEC Campus, 17 rue des Martyrs, F-38054 Grenoble, France
[c] CEA, INES, 50 avenue du Lac Léman, F-73377 Le-Bourget-du-Lac, France

ARTICLE INFO

Article history:
Received 30 November 2016
Received in revised form 19 June 2017
Accepted 19 June 2017
Available online 24 June 2017

Keywords:
Ion implantation
Photovoltaic
Beam Line
Plasma Immersion

ABSTRACT

Production costs and energy efficiency are the main priorities for the photovoltaic (PV) industry (COP21 conclusions). To lower costs and increase efficiency, we are proposing to reduce the number of processing steps involved in the manufacture of N-type Passivated Rear Totally Diffused (PERT) silicon solar cells. Replacing the conventional thermal diffusion doping steps by ion implantation followed by thermal annealing allows reducing the number of steps from 7 to 3 while maintaining similar efficiency.

This alternative approach was investigated in the present work. Beamline and plasma immersion ion implantation (BLII and PIII) methods were used to insert n-(phosphorus) and p-type (boron) dopants into the Si substrate. With higher throughput and lower costs, PIII is a better candidate for the photovoltaic industry, compared to BL. However, the optimization of the plasma conditions is demanding and more complex than the beamline approach.

Subsequent annealing was performed on selected samples to activate the dopants on both sides of the solar cell. Two annealing methods were investigated: soak and spike thermal annealing. Best performing solar cells, showing a PV efficiency of about 20%, was obtained using spike annealing with adapted ion implantation conditions.

1. Introduction

In the PV industry, the main challenge is to increase the efficiency of the solar cells while reducing the manufacturing costs. For this, the process flow must be optimized with a simplification, or a decrease of the number of the process steps.

In this study, we propose to change the traditional gas diffusion doping process by an ion implantation doping process. The ion implantation allows to better control the doping profile inside the material with a better uniformity and reproducibility [1]. Also it allows to reduce significantly the number of process steps. In future, this doping process will reach the new cell technologies such as Interdigitated Back Contact (IBC) or selective emitter cells. The first tests on silicon solar cells using ion implantation date from 1980, where encouraging yields were reached [2]. Nevertheless, this doping technology is not very used in the PV industry, besides in microelectronic industry, because up to now, the ion implantation tools were relatively expensive and the throughput was not adapted to the PV industry. These last years, the development of the ion implantation technologies, such as Beam Line, Plasma Immersion or Shower, has consented to reduce the price of the ion implantation tools and to increase the throughput to become competitive for the PV industry.

In this paper we investigated the n-type and p-type doping for the fabrication of N-type homojunction silicon solar cells using ion implantation followed by an activation annealing. Our study consisted on comparing Beam Line Ion Implantation (BLII) versus plasma immersion ion implantation (PIII) techniques and also Soak annealing versus Spike annealing techniques. Firstly, we have separately optimized and electrically characterized the doping process of each type. Thus, these optimized doping processes were integrated on the total process flow for the fabrication of entire solar cells.

2. Experimental

In the PV industry, there are two cell technologies: Homojunction & Heterojunction, with different cell architectures. In our study, we used homojunction N-type implanted Passivated Rear Totally Diffused (PERT) silicon solar cells. N-type silicon has many

* Corresponding author at: CEA, LETI, MINATEC Campus, 17 rue des Martyrs, F-38054 Grenoble, France.
E-mail address: frederic.milesi@cea.fr (F. Milési).

http://dx.doi.org/10.1016/j.nimb.2017.06.020
0168-583X/

advantages like the absence of light induced degradation (LID) [3,4], a low sensitivity to metallic impurities and a high lifetime potential [5]; and PERT architecture conciliates high efficiency and cost effective ($/W) processes [6].

A schematic cross-section view of this Si(n)-based cell is presented in Fig. 1. It is composed of an emitter in the front side doped with boron (B) and a back surface field (BSF) in the back side doped with phosphorus (P). Then the cell is passivated with SiO_2 and SiN_x layers. The last one is also used as antireflective coating. Finally, the front and rear contacts are fabricated using screen printing metallization.

Fig. 2 presents a simplified process flows for the fabrication of n-type cells using diffusion or ion implantation. In each flow, the steps corresponding to doping (ion implantation and thermal annealing) are highlighted in green boxes. In gaseous diffusion method, the cell is doped using the standard thermal diffusion process. However, such approach demands the deposition of a physical barrier to protect the rear side during front side diffusion and the front side during rear side diffusion. A last thermal oxidation step is needed for surface passivation. While in ion implantation method, the dopants are inserted into the cell by ion implantation and activated by subsequent thermal treatments. In these approaches, the number of process steps related to doping is reduced by 4 [7], in comparison to the 7 steps needed for doping by diffusion. Using ion implantation, the steps of barrier and dopant glass removal are eliminated and the oxidation is done during the activation annealing.

The substrates used in this study were 239 cm^2 Czochralski n-type pseudo-square silicon wafers with a thickness of 180 μm.

BLII were done using a VIISTA HCP of Applied Materials, and PIII were performed in Pulsion™ Nano from Ion Beam Services (IBS). Both tools are 300 mm micro-electronic ion implanters where we developed special silicon PV holders in order to process PV wafers as well as 300 mm wafers with no soft or hardware modifications. In BLII, the ion implantation parameters to define the dopant profile in the material are the specie, the energy (keV) and the dose (at/cm^2). While in PIII, in addition to the ion implantation parameters, the plasma parameters (gas precursor, RF power, chamber pressure, gas flow, time of pulse) have also an importance on the dopant profile. It is a technology more complex to apprehend, so first of all, we focused on the study of the influence of plasma parameters through some Design Of Experiments (DOE).

The post-ion implantation activation annealing was performed in a horizontal furnace for the Soak annealing, with some up/down ramps around 5 °C/min, and in a Rapid Thermal Annealing (RTA) lamp furnace for the Spike annealing with some up/down ramps around 10 °C/s. The annealing parameters we explored were the temperature and the time of the annealing.

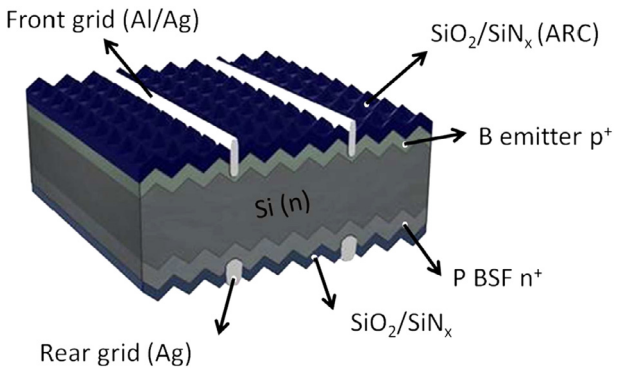

Fig. 1. Scheme in cross section view of a n-type PERT solar cell.

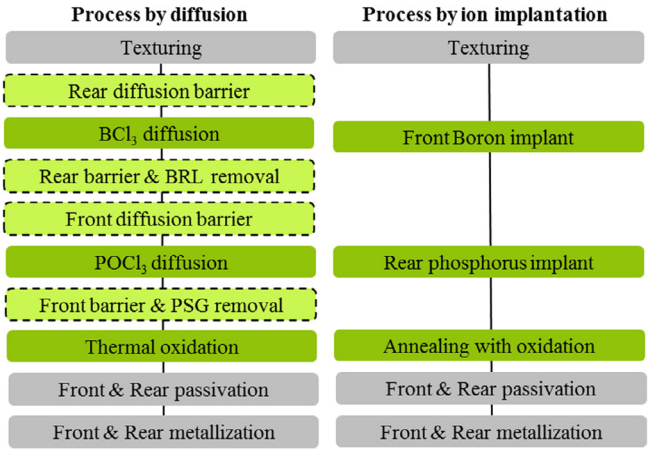

Fig. 2. Scheme of the process flows used to fabricate n-type Si solar cells: by diffusion or by ion implantation.

Firstly, we separately optimized the implantation and annealing conditions of the boron emitter and the phosphorus Back Surface Field (BSF), to obtain sheet resistance values similar from those of gas diffusion. Then, symmetrical cells with the same implantation and annealing conditions for both sides were fabricated. Finally, based on the results of the symmetrical cells, the best conditions of emitter and BSF were integrated in a solar cell.

In front side, an important dopant concentration in surface is necessary to have a good contact. However, a high doping concentration leads to the increase of Auger recombination rate, which limits the lifetime and the ultimate efficiency of the solar device. In rear side, the Back Surface Field (BSF) aims to repel the minority carriers in the bulk to minimize the impact of rear surface recombination. To fabricate the boron emitter in front side and the BSF in back side, ions were implanted with energies up to 10 keV and with a range dose from 10^{14} to 10^{15} at/cm^2. To activate both sides, annealing were performed at different temperatures, between 800 and 1050 °C during 1–60 min, with an included oxidation step for surface passivation.

All doped samples were characterized. Four probe method was used to measure sheet resistance after dopant activation. Secondary ion mass spectrometry (SIMS) analyses were done to obtain concentration-depth profiles of B emitter and P BSF. Electrocapacitance chemical voltage (ECV) was used to quantify the active amount of dopant as a function of depth.

To characterize symmetrical cells, lifetime measurement was done by quasi steady state photoconductance (QSSPC) where the implied open circuit voltage (iV_{OC}) and the saturation current density (J_{0e}) were determined. I/V measurements were performed to characterize the final cell and extract its efficiency.

3. Results and discussion

3.1. Diffusion

Since the beginning of the PV industry, the standard doping process is the diffusion on the both sides of the cell. It is a mature process where it is difficult to control the concentration and depth of the profile. Moreover, it is a technology that is not adapted to all cell architectures. The fact of tuning only diffusion parameters like temperature, time and gas flow, does not allow reaching cell efficiencies beyond 20% in production.

Fig. 3 shows SIMS profiles, which are the chemical profiles and ECV profiles, which are the activated profiles of the dopants for the

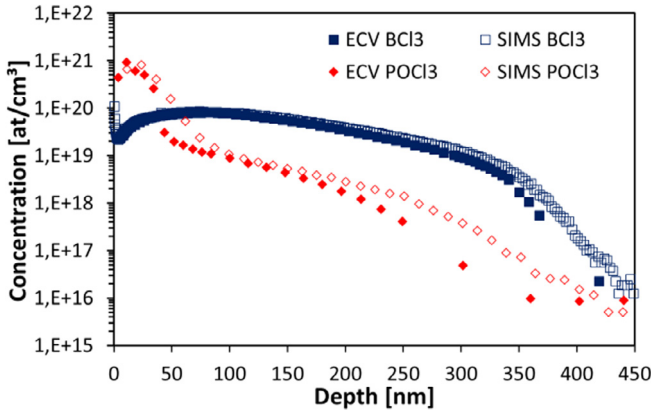

Fig. 3. Boron & phosphorus concentration-depth SIMS profiles of emitter & BSF obtained by diffusion.

Table 1
Average QSSPC performances of symmetrical cells fabricated with diffusion technology.

Diffusion	QSSPC measurements		
	J0e (fA/cm^2)	iVOC (mV)	R^2 (Ω/sq)
BCl_3	98	658	85
$POCl_3$	135	665	75

Table 2
Average I(V) performances of solar cells fabricated with diffusion technology.

Process	I(V) measurements			
	JSC (mA/cm^2)	VOC (mV)	FF (%)	η (%)
Diffusion	38.9	646.8	79.5	20

emitter and BSF doping process by diffusion. By diffusion technology, almost all the introduced dopants are active.

Tables 1 and 2 summarize the average QSSPC and I/V measurements of symmetrical solar cells fabricated by diffusion with the emitter in BCl_3 and the BSF in $POCl_3$. These diffusion results will be used as a reference in the process improvement and in the process steps reduction obtained with ion implantation technology.

3.2. Beam Line Ion Implantation (BLII)

3.2.1. Emitter fabrication

To obtain a similar sheet resistance to the diffusion process, there are many implantation (dose and energy) and annealing parameters (temperature and time) which can be tuned. For boron activation, temperatures above 950 °C are necessary to fully activate implanted boron atoms and to recover implantation damages [8]. The impact of the annealing temperature on the emitter quality was studied for various implantation doses on symmetrical cells.

Fig. 4a) shows the R_{sheet} measured on samples implanted at different doses and annealed at 950 °C and 1050 °C. As expected, it is observed that R_{sheet} strongly decreases for increasing implantation doses, whatever the annealing temperatures. This behavior is explained by an augmentation of the active boron concentration due to the higher implantation dose. The difference on R_{sheet} between both annealing temperatures, observed for the lowest implantation doses, can be explained by the change in carrier mobility [9].

Fig. 4b) shows the J_{0e} values measured on these same samples. For the lowest implantation dose, very low J_{0e} values (under 20 fA.cm^{-2}) were obtained for both annealing temperatures. This result indicates a complete activation of implanted boron atoms and the recovery of implantation damages. For the highest implantation dose, only the high temperature 1050 °C annealing renders a low J_{0e} value. This is because the implantation defects are annealed out and there is no significant Shockley-Read-Hall (SRH) recombination in the emitter, meaning that there are no impurities and no crystalline defects. At 950 °C, the higher J_{0e} is due to recombination defects like inactive boron, boron interstitial clusters (BICs) or intrinsic defects like dislocation loops causing J_{0e} degradation [8]. They confirm that for the formation of a boron emitter with high electrical quality that is suitable for contact by screen-printing metallization, a 1050 °C annealing is strongly recommended.

The depth-concentration profile of the emitter implanted with the optimized B condition and subsequently activated with Soak annealing was obtained by SIMS. The result is presented in Fig. 5 together with the concentration-depth profile of the B emitter activated by diffusion, for comparison purposes. The post implantation annealing resulted in a B profile (triangles) with lower surface concentration and higher depth penetration than the standard B emitter obtained by diffusion (squares).

3.2.2. BSF fabrication

Previous results showed that to obtain some similar diffusion results for the boron emitter, we have to implant with high implantation doses (10^{15} at/cm^2) and to anneal at high temperature. A 1050 °C thermal treatment is needed to activate the boron emitter during solar cell fabrication. Thereafter, this temperature must be also used for the P-BSF activation. The impact of this high annealing temperature on the P-BSF quality was studied and the obtained results are presented in this section.

Like boron, the sheet resistance of implanted phosphorus decreases with the increase in annealing temperature (for the same

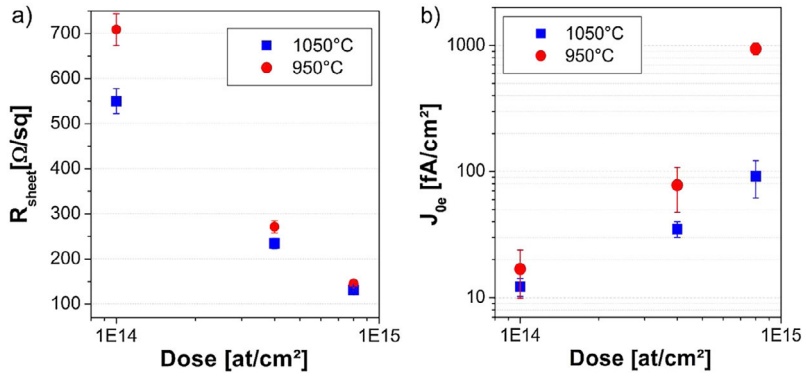

Fig. 4. a) R_{sheet} and b) J_{0e} as a function of implantation dose. The measurements were carried out in implanted symmetrical samples annealed at T_p = 950 °C and T_p = 1050 °C [10].

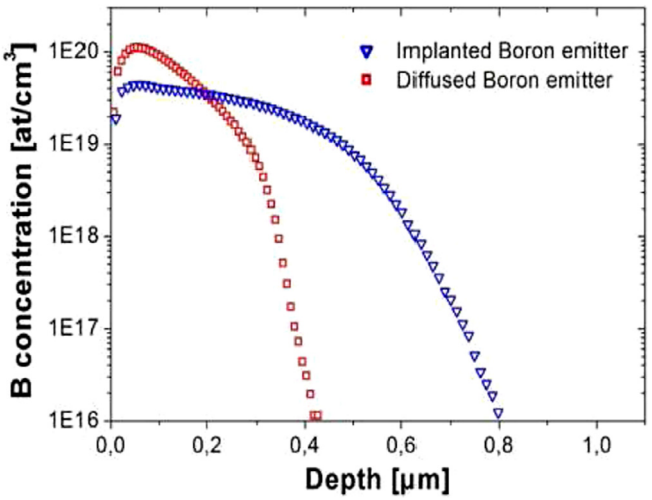

Fig. 5. Boron concentration-depth SIMS profiles of emitters obtained by implantation plus soak annealing and by diffusion [11].

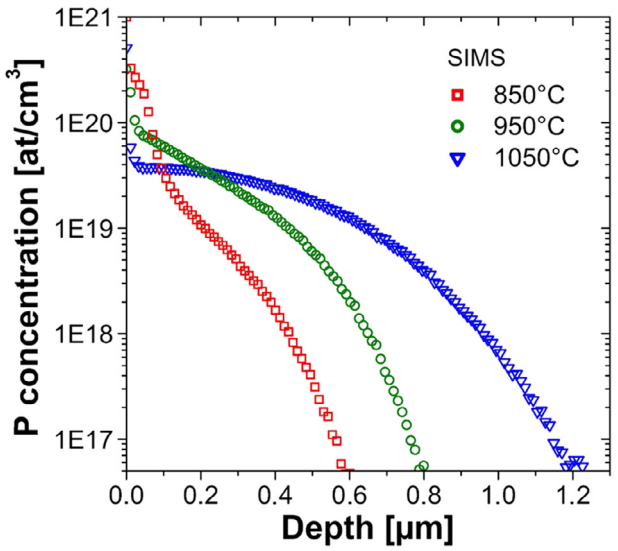

Fig. 6. Phosphorous concentration-depth profiles obtained by SIMS for samples annealed for 1 h at different temperatures and followed by an oxidation step [10].

ion implantation conditions), but the phosphorus concentration profile changes. Fig. 6 shows phosphorus profiles for several annealing temperatures. By increasing temperature, we observe a decreased surface doping and an increased depth penetration. Therefore the R_{sheet} decrease is only due to an increase of the carrier mobility for less concentrated profiles [11]. Actually, as it was highlighted in our previous work on p-type silicon solar cells [12], all the phosphorus atoms are already activated at 850 °C.

3.2.3. Solar cells

The optimized processes for the Emitter and for the BSF with a 1050 °C annealing were used to fabricate symmetrical cells, which the results are summarized in the Table 3. Thus, solar cells were actually manufactured. For the symmetrical cells, the implantation results are similar than diffusion but the final cell efficiency is lower (Table 4). This result is due to a low Fill Factor (FF), which limits the yield (by resistive losses and parasite currents). This effect is caused by a low P surface concentration leading to a bad contact in surface (see Table 5).

Table 3
Average QSSPC performances of symmetrical cells fabricated by implantation technology and compared with diffusion technology.

Process	QSSPC measurements		
	J0e (fA/cm^2)	iVOC (mV)	R^2 (Ω/sq)
BCl_3 by Diffusion	98	658	85
B by Implantation	120	670	88
$POCl_3$ by Diffusion	135	665	75
P by Implantation	90	670	85

Table 4
Average I(V) performances of solar cells fabricated by implantation technology and compared with diffusion technology.

Process	I(V) measurements			
	JSC (mA/cm^2)	VOC (mV)	FF (%)	η (%)
Diffusion	38.9	646.8	79.5	20
Implantation	39.1	650.6	77.3	19.7

Table 5
Average I(V) performances of solar cells fabricated with three different dopant activation processes.

Process	I(V) measurements			
	JSC (mA/cm^2)	VOC (mV)	FF (%)	η (%)
Separated annealing	39.1	651.5	79.1	20.2
Co-annealing	39.1	650.6	77.3	19.7
Diffusion	38.9	646.8	79.5	20

Table 6
Average QSSPC performances of P BSF symmetrical cells fabricated by Spike and Soak annealing, and compared with diffusion technology.

Annealing	QSSPC measurements		
	J0e (fA/cm^2)	iVOC (mV)	R^2 (Ω/sq)
Spike	155	646	72
Soak	90	670	85
Diffusion	135	665	75

With one single annealing at 1050 °C, (called co-annealing), we have a good boron activation but an important phosphorus diffusion. To improve the surface contact and to limit the phosphorus diffusion, different ways were explored in order to increase the solar cell efficiency (see Table 6).

3.2.3.1. Separated annealing. One possible solution to limit P diffusion is to separate the emitter annealing and the BSF annealing, by adding one step. For this, we performed an adapted annealing for each dopant. For boron activation, we used a 1050 °C annealing and for phosphorus activation, an annealing lower than 950 °C.

The results of ECV measurements are presented in Fig. 7. The concentration of activated P as a function of its depth is plotted for the co-annealing, the separated annealing and the diffusion activation processes.

The profile of P atoms activated by co-annealing presents a lower surface concentration and higher depth penetration compared to the concentration-depth profiles of P atoms activated by separated annealing and by diffusion. A best efficiency is obtained using separated annealing process, with an average of 20.2%, i.e. 0.2% more efficiency than the standard cell fabricated by diffusion. The record cell was obtained with a yield of 20.33% [14] (certified by the Fraunhofer CalLab).

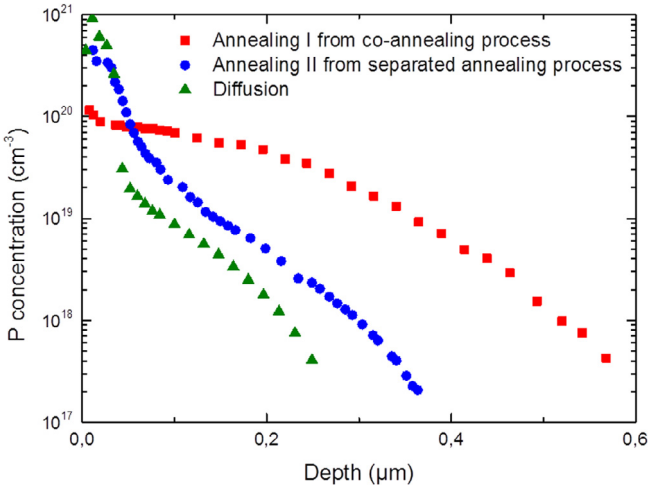

Fig. 7. Concentration-depth ECV profiles of P BSF doped by implantation and activated by co-annealing and separated annealing, and P BSF activated by diffusion [13].

3.2.3.2. Spike annealing. Another way to improve the surface contact and to limit the phosphorus diffusion is to change the annealing type. Replacing the soak annealing by a spike annealing and a 1050 °C annealing is possible to activate boron and phosphorus without phosphorus diffusion. In this case, there is no additional step and compared to the soak annealing, the up/down ramps are sharper leading to less dopant diffusion.

Fig. 8 show the concentration-depth ECV profiles of P BSF. We observe a higher phosphorus concentration at the surface for the Spike annealing similar than diffusion but the emitter density current J0e is too high and the implied carrier concentration Voc is too low. There are two possibles explanations for this phenomenon: either the total thermal budget is too low to repair the total implant damages, or the up/down ramps are too abrupt. Some works are in progress to improve the J0e and iVoc with the Spike annealing with a longer process time, or a softer up/down ramp.

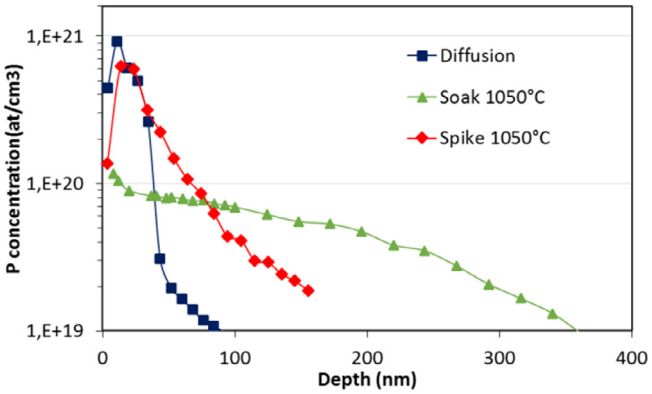

Fig. 8. Concentration-depth ECV profiles of P BSF doped by implantation and activated by soak and spike annealing, and P BSF activated by diffusion.

Table 7
Average QSSPC performances of BSF symmetrical cells fabricated by arsenic ion implantation, and compared with phosphorus ion implantation and diffusion technology.

BSF Process	QSSPC measurements		
	J0e (fA/cm^2)	iVOC (mV)	R^2 (Ω/sq)
As Implantation		620	
P Implantation	90	670	85
Diffusion	135	665	75

3.2.3.3. Arsenic dopant. Another solution for BSF fabrication is to substitute phosphorus by arsenic. As is also a p-type dopant that diffuses less than P but which generates more damages in the material after ion implantation. The firsts results on symmetrical cells, shown in the Table 7, reveal that the additional damage introduced by the arsenic degraded iVoc results.

3.3. Plasma immersion ion implantation (PIII)

As showed in the previous section, good cell results were obtained with beam line ion implantation. For the implantation technique to be competitive, ion implantation processes by plasma immersion should be developed because this technology is more adapted to the PV industry, with a lower purchase price and a higher throughput (more important dose rate, no beam scanning and higher surface implantation).

Even if plasma implanters are simpler, processes are more complex to develop. In fact, in PIII a large number of parameters such as precursor gas, gas flow, chamber pressure, RF power, use of pulsed or continuous process and so on can have an influence on the final implanted species profile and dose.

To illustrate the plasma doping complexity, two boron profiles obtained by SIMS analyses are presented in Fig. 9, where B concentration is plotted as a function of depth. The same energy and "machine" dose were used for both boron implantations using B_2H_6 gas precursor.

In fact, a major difference between BLII and PIII is the absence of mass selection in the later, meaning that all the positive ions in the plasma are implanted into the target ($BF^+_{x<3}$, B^+, F^+ ions with BF_3; $B_2H^+_{x<6}$, B^+, BH^+_x with B_2H_6; $PH^+_{x<3}$, P^+ with pH_3). Thus, the total dose implanted in the sample is the sum of all positive ions present in the precursor gas, independent if they are the desired dopants or not. This total implanted dose is called "machine dose" and can be very different from the dose of one specific dopant specie. For this reason, plasma processes must be optimized. Thus, Designs of Experiments (DOE) were performed on plasma parameters for the different precursor gases.

3.3.1. Boron emitter fabrication

The conventional gas used in BLII to perform some p-type dopants is the BF_3. So for the plasma immersion, we decide to use BF_3 as gas precursor to fabricate the emitter. Whatever the plasma immersion process and the soak annealing conditions, we

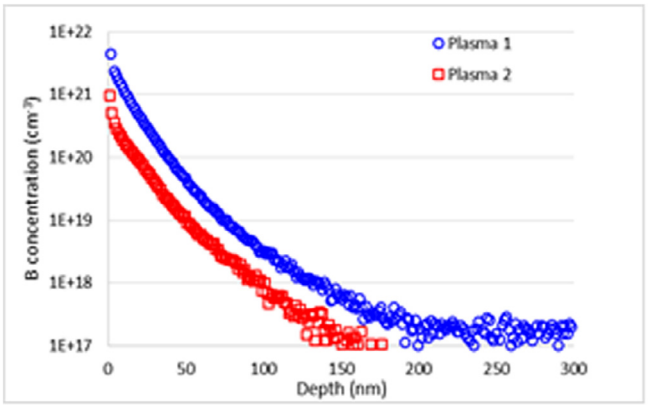

Fig. 9. B concentration-depth profiles measured by SIMS for B_2H_6 ion implantation at 10 keV with dose machine = 3.5×10^{15} at/cm^2.

Table 8
Impact of the co-implantation of fluorine on the iV_{OC} and J_{0e} values.

Emitter Process	QSSPC measurements	
	iV_{OC} (mV)	J_{0e} (fA.cm^{-2})
B in BLII	670	120
BF_3 in PIII	620	190
BF_2 in BLII	607	190

Table 9
Comparison of iV_{oc} and J_{0e} values for different boron emitters.

Emitter Process	QSSPC measurements	
	iV_{OC} (mV)	J_{0e} (fA.cm^{-2})
B in BLII	670	120
BF_3 in PIII	620	190
B_2H_6 in PIII	669	99

Table 10
Comparison of iV_{oc} and J_{0e} values for different phosphorus BSF.

Process	iV_{OC} (mV)	J_{0e} (fA.cm^{-2})	R_{sheet} (Ω/sq)
P in BLII	670	90	85
pH_3 in PIII	670	92	82

Table 11
Performances of n-type hybrid PERT cells.

Process	I(V) measurements			
	JSC (mA/cm^2)	VOC (mV)	FF (%)	η (%)
Record cell	39.2	650.3	77.7	19.8
Average (15 cells)	39.2	648.0	77.3	19.6

obtain the same range characteristics on symmetrical cells, as BLII emitter for the sheet resistance and J_{0e}. On the other side, the implied carrier concentration iV_{oc} remains limited to 630 mV [13].

To understand these results, BF_2^+ ions were implanted on symmetrical cells using BLII to mimic the PIII technique where BF_2^+ ions constitute the majority of the implanted species [15–17]. The results are summarized in Table 8.

Even though the low emitter saturation current density J_{0e} values (<200 fA.cm^{-2}) validate the quality of the space charge zone and give an indication on the complete boron activation, BF_2^+ emitters are limited by the low iV_{OC}, like for the BF_3 emitters. We attributed this result to the co-implantation of fluorine inducing, after high thermal annealing, a significant degradation of the bulk lifetime. The reason for such degradation is not clearly established and can be due to deep defects after annealing and/or activation of recombination centers linked to the implantation of F atoms [18].

To avoid the co-implantation of F atoms and its compounds, diborane (B_2H_6) was tested as boron gas precursor. Like before, we have the same range characteristics on symmetrical cells, for the sheet resistance and J_{0e}, but this time, iV_{OC} values are close to those obtained by B^+ implantation using the BLII technique (shown in the Table 9).

3.3.2. BSF fabrication

Phosphorus implantation by PIII technique has already shown good results on p-type silicon solar cells with an efficiency improvement of 0.7% only replacing $POCl_3$ diffusion by pH_3 implantation [19].

Compared to the emitter boron PIII process, there was less process development for the BSF fabrication. We went from the BLII to the PIII keeping the same implantation energy and dose. Good electrical results were obtained on symmetrical cells. These results are shown in Table 10, where the values obtained with PIII and BLII are the same.

3.3.3. Solar cells

To validate the optimum B_2H_6 emitter, n-type PERT silicon solar cells were fabricated. Such cells are called "hybrid cell", where the emitter fabrication was done by B_2H_6 plasma immersion and the BSF by phosphorus beam line. Dopants were activated using a Soak separated annealing. Cells performances are summarized in Table 11 [20]. A maximum efficiency of 19.8% was reached. Averaged results on the full batch of 15 cells show excellent reproducibility.

In the aim to only use PIII technique, the first developments of B_2H_6 emitter and pH_3 BSF by PIII were integrated on cells. The first results allow to reach a maximum efficiency of 18.8%. To our knowledge, this is the first promising result published about n-type PERT solar cells fully doped by PIII. More works must be done to reach around 20% of efficiency.

4. Conclusion

In this work we studied the doping of n-type silicon solar cells using two ion implantation techniques: BLII and PIII, allowing to reduce the number of doping process steps for the n-type PERT silicon solar cells, from 7 to 3. Compared to the diffusion techniques, we obtained a record cell of 20.33% efficiency using BLII doping and separated Soak annealing.

In PIII, we developed boron emitter using B_2H_6 as precursor gas. Hybrid cells combining PIII for emitter doping and BLII for BSF reached 19.8% efficiency.

In the future, the ideal industrial technology for the fabrication of n-type PERT silicon solar cells will be to combine plasma immersion ion implantation on both sides (emitter by B_2H_6 and BSF by pH_3) with the Spike annealing. For this, we studied all the different steps (BLII + Soak, BLII + Spike, PIII + Soak and PIII + Spike) to reach this ideal technology. We have yet to develop the Spike annealing process to improve the low emitter saturation current density J_{0e} and we have to optimize the BSF pH_3 plasma immersion to improve the implied carrier concentration iV_{oc}. Some works are in progress to improve the different technologies, but cells fully doped by PIII and soak annealed were already fabricated and a yield of 18.8% was obtained. These first results are encouraging for the continuation of the development of the PIII and Spike technologies.

Acknowledgments

This work was done under the LETI/INES collaboration on the process development of solar cell doping by ion implantation.

References

[1] A. Rohatgi et al., High throughput ion implantation for low cost high efficiency silicon solar cells, Energy Procedia 15 (2012) 10–19.
[2] M.B. Spitzer, S.P. Tobin, C.J. Keavney, High efficiency ion implantation silicon solar cells, IEEE Trans. Electron Devices 31 (1984) 546–550.
[3] K. Bothe, J. Schmidt, Electronically activated boron-oxygen-related recombination centers in crystalline silicon, J. Appl. Phys. 99 (1) (2006) 013701.
[4] B. Sopori et al., Understanding light-induced degradation of c-Si solar cells, in: 38th IEEE Photovoltaic Specialists Conference, 2012, pp. 1115–1120
[5] D. Macdonald, L.J. Geerligs, Recombination activity of interstitial iron and other transition metal point defects in p- n-type crystalline silicon, Appl. Phys. Lett. 85 (18) (2004) 4061–4063.
[6] R. Kopecek, J. Libal, The status and future of industrial n-type silicon solar cells, Photovoltaics Int. (2013).

[7] A. Lanterne et al., High efficiency fully implanted and co-annealing bifacial n-type solar cells, Energy Procedia 38 (2013) 283–288.
[8] R. Müller et al., Evaluation of implantation annealing for highly-doped selective boron emitters suitable for screen-printed contacts, Sol. Energy Mater. Sol. Cells 120 (2014) 431–435.
[9] G. Masetti, M. Severi, S. Solmi, Modeling of carrier mobility against carrier concentration in arsenic-, phosphorus-, and boron-doped silicon, IEEE Trans. Electron Devices 30 (17) (1983) 764–769.
[10] A. Lanterne et al., Understanding of the annealing temperature impact on ion implanted bifacial n-type solar cells to reach 20.3% efficiency, Prog. Photovoltaics Res. Appl. (2014).
[11] A. Lanterne et al., Diffused and implanted boron emitter toward high efficiency n-type PERT solar cells, presented to the 3rd nPV workshop, Chambéry, France, 2013.
[12] A. Lanterne et al., Annealing, passivation and contacting of ion implanted phosphorus emitter solar cells, Energy Procedia 27 (2012) 580–585.
[13] M. Coig et al., Solar cells doping by beam line and plasma immersion ion implantation, in: Proceedings Ion Implantation Technology (IIT) conference, 2014
[14] A. Lanterne et al., 20.5% efficiency on large area n-type PERT cells by ion implantation, in: 4th International Conference on Silicon Photovoltaics, SiliconPV, 2014.
[15] V. Kaeppelin et al., Characterization of an industrial plasma immersion ion implantation reactor with a Langmuir probe and an energy-selective mass spectrometer, Surf. Coat. Technol. 156 (2002) 119–124.
[16] B.W. Koo et al., Plasma diagnostics in pulsed plasma doping (P2LAD) system, IEEE Trans. Plasma Sci. 32 (2004) 453–456.
[17] A. Burenkov et al., Simulation of BF3 plasma immersion ion implantation into silicon, AIP Conf. Proc. 1496 (2012) 233.
[18] A. Lanterne et al., Solar-grade boron emitters by BF3 plasma doping and role of the co-implanted fluorine, Prog. Photovoltaics Res. Appl. (2015).
[19] J. Le Perchec et al., 19.3% efficiency on p-type silicon solar cells by Pulsion® plasma immersion implantation, Energy Procedia 33 (2013) 18–23.
[20] J.-F. Lerat et al., Boron emitter formation by plasma immersion ion implantation in n-type PERT silicon solar cells, in: 6th International Conference on Silicon Photovoltaics, SiliconPV, 2016.